Staggered and moving localized modes in dynamical lattices with the cubic-quintic nonlinearity

Aleksandra Maluckov*
Faculty of Sciences and Mathematics, University of Niš, P.O. Box 224, 18001 Niš, Serbia

Ljupčo Hadžievski
Vinča Institute of Nuclear Sciences, P.O. Box 522, 11001 Belgrade, Serbia

Boris A. Malomed
Department of Physical Electronics, School of Electrical Engineering, Faculty of Engineering, Tel Aviv University, Tel Aviv 69978, Israel
(Received 8 November 2007; published 7 March 2008)

Results of a comprehensive dynamical analysis are reported for several fundamental species of bright solitons in the one-dimensional lattice modeled by the discrete nonlinear Schrödinger equation with the cubic-quintic nonlinearity. Staggered solitons, which were not previously considered in this model, are studied numerically, through the computation of the eigenvalue spectrum for modes of small perturbations, and analytically, by means of the variational approximation. The numerical results confirm the analytical predictions. The mobility of discrete solitons is studied by means of direct simulations, and semianalytically, in the framework of the Peierls-Nabarro barrier, which is introduced in terms of two different concepts, free energy and mapping analysis. It is found that persistently moving localized modes may only be of the unstaggered type.

DOI: 10.1103/PhysRevE.77.036604 PACS number(s): 05.45.Yv, 63.20.Ry, 42.65.Tg, 03.75.Lm

I. INTRODUCTION

A broad class of lattice models in various fields of physics is described by discrete nonlinear Schrödinger (DNLS) equations [1]. A direct realization of the DNLS model with the cubic on-site nonlinearity in arrays of optical waveguides was predicted in Ref. [2], and later demonstrated experimentally in a structure built as a set of parallel semiconductor waveguides mounted on a common substrate [3,4]. Multichannel waveguiding systems can also be created in a *virtual* form, as photonic lattices in photorefractive crystals [5]. In the DNLS equation with the simplest cubic nonlinearity, a number of fundamental dynamical phenomena have been studied, both experimentally (in the above-mentioned optical settings) and theoretically. These include the mobility [6,7] and collisions of discrete solitons [7,8], as well as the onset of the spatiotemporal collapse in an array of self-focusing waveguides [9]. It was also demonstrated theoretically and experimentally that the DNLS equation is an adequate model for the Bose-Einstein condensate (BEC) trapped in a deep optical lattice, which effectively splits the condensate into a set of "droplets" captured in local potential wells and coupled linearly through tunneling of atoms [10].

The ordinary DNLS equation includes cubic nonlinear terms (alias the Kerr nonlinearity, in terms of optics). A more general discrete cubic nonlinearity appears in the Salerno model [11], which combines the onsite cubic terms and ones that account for nonlinear coupling between adjacent sites (i.e., it is a combination of the DNLS and Ablowitz-Ladik [12] systems). In addition to the ordinary Salerno model, its modification featuring competing onsite and intersite cubic nonlinearities was explored too [13].

More general dynamical lattice models involve non-Kerr nonlinearities. In particular, the first discrete system with saturable onsite nonlinear terms was introduced in 1975 by Vinetskii and Kukhtarev [14]. Stable bright solitons in this model were reported only recently in Ref. [15] [two-dimensional (2D) discrete solitons in a model with the saturable nonlinearity were studied also [16]]. Experimentally, lattice solitons supported by the saturable self-defocusing nonlinearity were created in an array of optical waveguides in a photovoltaic medium [17].

The availability of optical media whose effective nonlinearity may be represented as a combination of the self-focusing cubic and self-defocusing quintic terms [18] (with an addition of two-photon absorption, i.e., a cubic dissipative term, which, however, may be neglected under certain conditions [19]) suggests considering soliton dynamics in models with the corresponding cubic-quintic (CQ) nonlinearity. In particular, a family of stable exact soliton solutions of the continuum NLS equation of this type (in the free space, i.e., without any external potential) is well known [20]. Further, the possibility of building a waveguide array, using materials whose nonlinear response is of the CQ type, makes it natural to introduce the DNLS equation with the onsite CQ nonlinearity. An intermediate step between the CQ equation in the free space and the discrete model is a continuum equation combining this nonlinearity and a periodic potential in the form of the Kronig-Penney lattice, i.e., a periodic chain of rectangular potential wells. Recently, stable families of bright solitons were explored in 1D [21] and 2D [22] versions of such a model (the latter one, which features a "checkerboard" 2D potential, supports both fundamental and vortical solitons). The limit case of the Kronig-Penney potential composed of very deep and narrow potential wells amounts to the replacement of the continuum equation by its DNLS counterpart.

*maluckov@junis.ni.ac.yu

Another realization of the CQ-DNLS model is possible in a self-attractive BEC, which may be confined, in plane (x,y), by a combination of a two-dimensional (2D) "pancake"-shaped trap and a very strong quasi-2D optical-lattice potential, which is uniform along axis z. In the first approximation, the BEC trapped in each individual elongated (along z) potential well of this configuration is described by the 1D Gross-Pitaevskii equation with the CQ nonlinearity, the extra quintic term accounting for the deviation of the well's shape from one-dimensionality [23] (a more accurate analysis yields a nonpolynomial nonlinearity, whose lowest-order expansion generates the cubic and quintic terms [24]). Then, the tunneling of atoms between adjacent potential walls gives rise to the linear coupling between sites of the effective dynamical lattice. The difference of the thus introduced CQ lattice model from the one emerging in nonlinear optics (see above) is that the quintic term appearing in the context of the BEC is *self-focusing* (as well as its cubic counterpart), i.e., the nonlinearity does not have the competing character. It is relevant to mention that the quantum version of the DNLS equation (the Bose-Hubbard model) with the CQ nonlinearity and periodic boundary conditions was introduced too [25].

Thus the study of discrete solitons in the DNLS equations with the onsite nonlinearity of CQ type is a relevant physical problem. Recently, the simplest bright solitons, of the *unstaggered* type (without spatial oscillations in the solitons' tails), have been studied in detail in the 1D version of this model [26]. It was found that this class of the solitons includes infinitely many families that differ by their symmetry. The stability of the basic families and bifurcations linking them were explored, by means of numerical methods and variational approximation. It is relevant to mention that previous studies of bright solitons in the DNLS equation were dealing not only with the cubic nonlinearity [1], but also with nonlinear onsite terms of an arbitrary power [27]. Comparison with the results reported in Ref. [26] demonstrates that the competition between self-focusing cubic and self-defocusing quintic terms leads to a drastic change in the character of the solitons' states. Dark solitons in the CQ DNLS equation were recently investigated too, including ones supported by both unstaggered and staggered background fields [i.e., continuous waves (CWs)] [28].

The objective of this work is to study fundamental bright solitons in the CQ-DNLS equation (in 1D), focusing on soliton species that were not studied before, viz., ones of the staggered type, and moving solitons (both unstaggered and staggered). The model is formulated in Sec. II, and basic results for the existence of the discrete solitons are presented in Sec. III. In the same section, the rigorous stability analysis, based on computation of the eigenvalues for modes of small perturbations around stationary solitons, is elaborated. An essential goal of the work is the investigation of moving discrete solitons. To this end, the Peierls-Nabarro barrier (PNB) is introduced, in Sec. IV, in the framework of two concepts, viz., free energy, [28,29] and the mapping analysis [30,31]. The paper is concluded by Sec. V.

II. MODEL

The DNLS equation with the onsite CQ nonlinearity is taken in the usual form [26],

$$i\frac{d\psi_n}{dt} + C(\psi_{n+1} + \psi_{n-1} - 2\psi_n) + (2|\psi_n|^2 - |\psi_n|^4)\psi_n = 0, \quad (1)$$

where $\psi_n(t)$ is the field amplitude at the nth lattice site, C is the constant of the lattice coupling, and other coefficients are fixed by rescalings. In the above-mentioned optical realizations of the DNLS equation, evolution variable t represents not time, but the propagation distance in the waveguide array. Numerical solutions will be sought for below with periodic boundary conditions with respect to the discrete coordinate n ($\psi_n \equiv \psi_{n+N}$, where N is the full size of the lattice). Equation (1) conserves two dynamical invariants: power (norm) and Hamiltonian,

$$P = \sum_n |\psi_n|^2, \quad (2)$$

$$H = \sum_n \left[C\psi_n^*(\psi_{n+1} + \psi_{n-1} - 2\psi_n) + |\psi_n|^4 - \frac{1}{3}|\psi_n|^6 \right], \quad (3)$$

where $*$ stands for the complex conjugate. We will also use a combination of both invariants, namely, the free energy [28,29]:

$$G = H - \mu P. \quad (4)$$

Stationary solutions to Eq. (1) are looked for as $\psi_n(t) = u_n e^{ikn - i\mu t}$, where u_n is a real stationary lattice field, μ the frequency, and $k=0$ or $k=\pi$ refer to *unstaggered* and *staggered* stationary configurations, respectively. The substitution of this expression in Eq. (1) leads to a stationary equation,

$$\mu u_n + C(u_{n+1}e^{ik} + u_{n-1}e^{-ik} - 2u_n) + 2u_n^3 - u_n^5 = 0. \quad (5)$$

Two different types of both the unstaggered or staggered soliton solutions can be found from Eq. (5): On-site, with a maximum of the field at a particular lattice point, and intersite, formally centered at a midpoint between two adjacent lattice sites.

Unstaggered bright solitons generated by Eq. (5) were investigated in detail in Ref. [26], where multistable single-humped solutions of different symmetries were the central issue. First, they were found, and their stability was explored, by means of numerical methods at sufficiently small values of C. With the increase of C, stable antisymmetric solitons get destroyed through saddle-node bifurcations, while symmetric states pass a series of small pitchfork loops (cf. a bifurcation loop in a system of two linearly coupled continuum NLS equations with the CQ nonlinearity [32]). In addition, main branches of solutions and their bifurcations were reproduced, in the region of small C, in an analytical form by means of the variational approximation. In the same model, i.e., the DNLS equation with the CQ nonlinearity, dark solitons supported by the background (CW) lattice field of unstaggered and staggered types were studied in detail in Ref. [28], which included an analysis of the modulational stability of the CW fields. In particular, the staggered CW solution is modulationally unstable in interval $\mu > 4C-1$, offering the possibility for the creation of the staggered dark soliton.

In this paper we aim, first, to explore the stability of both unstaggered and staggered symmetric fundamental bright solitons in the CQ-DNLS model as a background for the main topic of the study of localized states moving across lattice. In this part of the paper, we focus on staggered stationary solitons, while results for unstaggered ones, which agree with what was reported in Ref. [26], are included in a brief form, with the intention to use them later in the study of moving solitons.

III. STABILITY OF DISCRETE BRIGHT SOLITONS

Some general conclusions concerning the stability of localized (bright) modes may be established on the basis of the energy-minimum or maximum principle, in the case of self-focusing or defocusing nonlinearity, respectively [33]. Recently, a modified principle based on the free energy was introduced [29] for systems close to an integrable limit. An example of that may be the above-mentioned Salerno system, which is close to the integrable Ablowitz-Ladik lattice model. In the case of the CQ focusing-defocusing nonlinearity, the relevance of the energy principle is not obvious (in this relation, it is relevant to mention that another general stability principle, viz., the Vakhitov-Kolokolov criterion [34], is *not* valid either for the continuum NLS equations with the competing CQ nonlinearity and periodic potential, in 1D and 2D settings alike [21,22]). In this work, we consider the stability of the bright soliton in two aspects: The eigenvalue spectrum, like in Refs. [26,28], and by means of mapping the orbital stability, following Ref. [30].

A. Eigenvalue spectrum

We examine the stability of the bright discrete solitons against small perturbations, adapting the method employed (for dark solitons) in Ref. [28]. To this end, solutions to Eq. (1), including an eigenmode of small perturbations, $\delta u_n \equiv \alpha_n + i\beta_n$, and the respective eigenvalue, λ, are looked for as

$$\psi_n = (u_n e^{ikn} + \delta u_n e^{\lambda t} e^{-i\kappa n}) e^{-i\mu t}, \tag{6}$$

where u_n represents the unperturbed real solution, $\kappa=0$ or $\kappa=\pi$ denote unstaggered or staggered perturbation, respectively, and the condition of the (marginal) stability being $\mathrm{Re}(\lambda)=0$. Then, the linearization leads to the eigenvalue problem based on the following equations,

$$\lambda \begin{pmatrix} \alpha_n \\ \beta_n \end{pmatrix} = \begin{bmatrix} 0 & H^+ \\ -H^- & 0 \end{bmatrix} \begin{pmatrix} \alpha_n \\ \beta_n \end{pmatrix} \equiv \mathbf{M} \begin{pmatrix} \alpha_n \\ \beta_n \end{pmatrix}, \tag{7}$$

where matrix $\mathbf{M}$ (of size $2N \times 2N$ for the lattice with N sites) is, generally, non-Hermitian. Elements of submatrices $H^{\pm}$ are

$$H^+_{jk} = [(2C-\mu) - 2u_j^2 + u_j^4]\delta_{jk} - C\cos(\kappa)(\delta_{j,k+1} - \delta_{j,k-1}),$$

$$H^-_{jk} = -H^+_{jk} + 4(2u_j^2 - u_j^4)\delta_{jk}. \tag{8}$$

Discrete eigenvalues of the matrix $\mathbf{M}$ determine the stability of the discrete solitons.

1. Unstaggered bright solitons

The stability spectrum for unstaggered solitons, numerically obtained in the entire existence region, contains pure imaginary and pure real eigenvalues, as shown in Fig. 1 in parameter plane (C,μ). In other words, the unstaggered discrete solitons are marginally stable, featuring only pure imaginary eigenvalues, or exponentially unstable, due to a pair of pure real eigenvalues. A noteworthy peculiarity of the region with small C (approximately, $C<0.15$) for unstaggered on-site and intersite states is the coexistence of two different symmetric fundamental solitons (with different values of the norm) at a fixed value of μ [26]. One of them has the amplitude smaller than 1, and the other one larger than 1. The corresponding stability eigenvalue spectra show that both solution branches of the on-site type are stable in the most part of the parameter plane, while the intersite mode with the amplitude smaller than 1 develops an exponential instability. The interchange of the stability between the on-site and intersite solitons, which have the same norm, with the variation of μ is clearly observed in Fig. 1 at medium and high values of C (approximately, at $C>0.15$); recall that the increase of C drives the system towards the continuum limit.

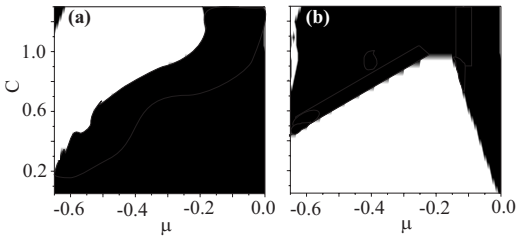

FIG. 1. Stability diagrams for unstaggered discrete solitons of the (a) on-site and (b) intersite types. Regions of the stability and exponential instability are depicted by black and white areas, respectively.

The evolution of those unstaggered solitons which are unstable is displayed in Fig. 2, for both small and large values of C. The proper interpretation of the instability development needs the knowledge of the corresponding $G(P)$ or $H(P)$ diagrams [recall that P, H, and G are defined in Eqs. (2)–(4)], see Fig. 3. Generally, the $G(P)$ [or $H(P)$] curves for the on-site and intersite states are close to each other at $C=0.8$, while at $C=0.05$ they are close only at small μ. This fact, and the smallness of the instability growth rate (the real eigenvalues are small), help to interpret the transformation of the unstable localized mode into a persistent localized breather, with approximately the same norm and (free) energy as the unstable soliton initially had, but localized around

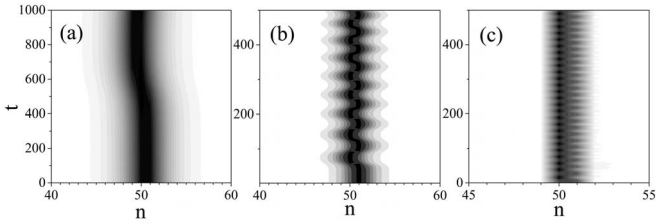

FIG. 2. Numerically simulated evolution of unstable unstaggered bright solitons: (a) and (b) the intersite type, for, severally, $C=0.8$, $\mu=-0.302$, and $C=0.05$, $\mu=-0.682$; (c) the on-site type, for $C=0.8$, $\mu=-0.602$.

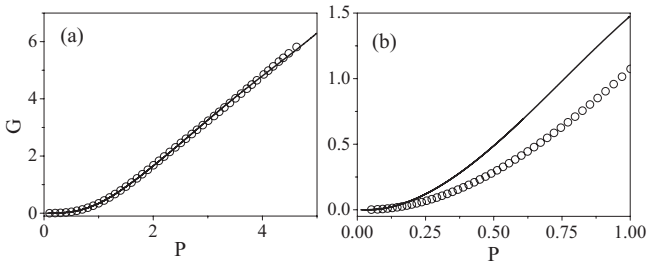

FIG. 3. Free energy vs total power for unstaggered bright solitons: (a) For $C=0.8$ and (b) for $C=0.05$. On-site and intersite states are represented by the solid curves and chains of circles, respectively.

an adjacent lattice site (in the case of an unstable intersite configuration), or between the initial and adjacent sites (in the case of unstable on-site configuration), as seen in Fig. 2.

2. Staggered bright solitons

Stability diagrams for staggered bright solitons, which, unlike the unstaggered ones, were not considered in Ref. [26], are displayed in Fig. 4, for (a) on-site and (b) intersite configurations. As seen from the figure, the on-site staggered discrete solitons are marginally stable in a wide region of the parameter plane. In the region of instability, the eigenvalue spectrum contains purely real eigenvalues; see Fig. 5(a). The resulting instability is strong, being triggered by large real eigenvalues, which leads to destruction of the soliton, as shown in Fig. 6(a).

On the other hand, the intersite staggered solitons may be subject not only to the exponential instability, but also to an oscillatory one, which corresponds to a pair of complex-conjugate eigenvalues; see Fig. 5(b). An example of the development of the corresponding oscillatory instability is shown in Fig. 6(b). The soliton sheds off a part of its norm, and is pinned at a nearby lattice site. On the contrary to the case of the unstaggered discrete solitons, the $G(P)$ or $H(P)$ curves for the on-site and intersite staggered states are widely separated, as seen in Fig. 7. Therefore, an unstable staggered soliton, either an on-site or intersite one, tends to

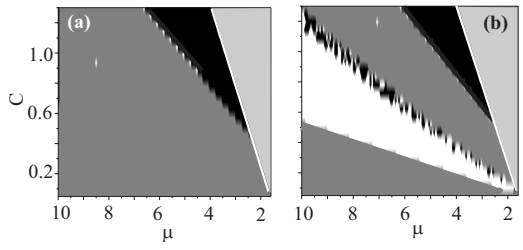

FIG. 4. Stability diagram for staggered bright solitons of the (a) on-site and (b) intersite types, in (μ, C) parameter plane. The regions of the stability, exponential instability, and oscillatory instability are represented by dark gray, black, and white areas, respectively. The numerically determined existence region of fundamental staggered solitons is located on the left from the white lines in both plots (in the light gray areas on the right of the white lines, the solitons do not exist).

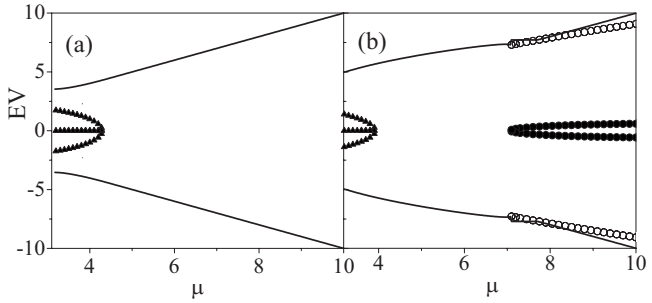

FIG. 5. Eigenvalue ("EV") spectrum for staggered bright solitons, of the (a) on-site and (b) intersite types, for $C=0.8$. Shown are purely imaginary (stable) eigenvalues with the largest absolute value (black lines), purely real (unstable) eigenvalues (triangles), and complex ones (black circles, the real part; open circles, the imaginary part).

transform itself into a stable state via emission of a considerable amount of the lattice radiation.

B. Variational approximation

Following Ref. [26], the VA (variational approximation) for the bright discrete solitons may be based on the exponential-cusp ansatz,

$$(u_n)_{\mathrm{VA}} = Ae^{-\alpha|n-n_0|}, \quad n_0 = n_c + \frac{1}{2}(\chi+1), \tag{9}$$

where amplitude A and inverse width α are real positive constants, with $\chi=0$ and $\chi=1$ for intersite and on-site configurations, respectively, and n_c is the coordinate of the central site of the soliton. Actually, α is not a variational parameter; instead, it is found by substituting ansatz (9) into the linearization of Eq. (5), i.e., it is taken from the consideration of the decaying tails of the soliton [26]:

$$\alpha = \ln\left[\frac{a}{2\cos k} + \sqrt{\left(\frac{a}{2\cos k}\right)^2 - 1}\right], \quad a \equiv 2 - \frac{\mu}{C}. \tag{10}$$

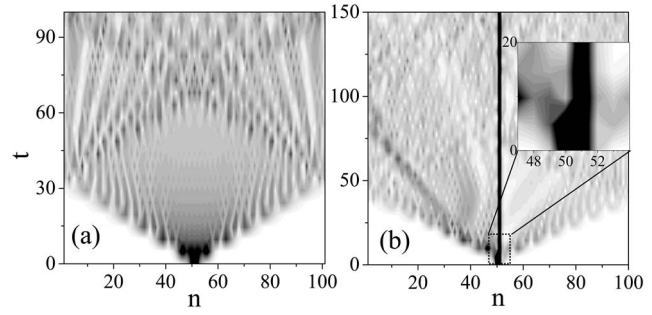

FIG. 6. Development of the instability of staggered bright solitons is shown by means of contour plots of the local amplitudes, $|\psi_n(t)|$: (a) For an unstable on-site state, with $C=0.8$, $\mu=3.545$; (b) for an intersite state, with $C=0.8$, $\mu=8.55$. The inset displays the initial stage of the mode evolution at the central lattice elements $n=[48,52]$.

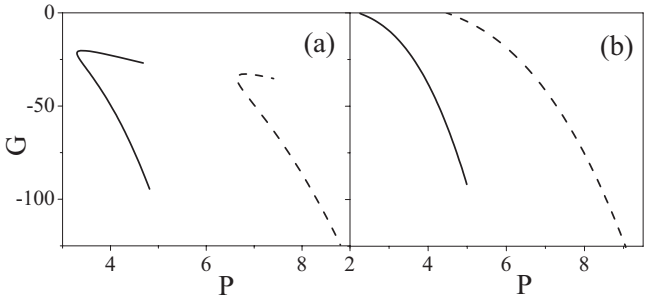

FIG. 7. Free energy vs total power for staggered bright solitons: (a) $C=0.8$; (b) $C=0.05$. On-site and intersite configurations are represented by solid curves and dashed curves, respectively.

Unlike α, amplitude A is treated as a variational parameter. For derivation of a variational equation for A, we use the Lagrangian corresponding to Eq. (5),

$$L = \sum_{n=-\infty}^{\infty} \left[(\mu - 2C)u_n^2 + u_n^4 - \frac{u_n^6}{3} + C\cos k(u_{n+1} + u_{n-1})u_n \right]. \tag{11}$$

Substitution of ansatz (9) in Eq. (11) yields the effective Lagrangian,

$$L_{\mathrm{VA}} = (\mu - 2C)A^2 S_0 + A^4 S_1 - \frac{A^6}{3} S_2 + 2CA^2 S_3 \cos k, \tag{12}$$

where we define

$$S_{j-1} \equiv \sum_{n=-\infty}^{\infty} e^{-2j\alpha|n-n_0|} = \frac{\cosh(j\alpha\chi)}{\sinh(j\alpha)}, \quad j = 1,2,3,$$

$$S_3 \equiv \sum_{n=-\infty}^{\infty} e^{-\alpha|n-n_0|-\alpha|n+1-n_0|} = \left[1 + \frac{\cosh(\alpha\chi)}{\sinh(\alpha)} \right] e^{-\alpha}.$$

The respective variational equation, $dL_{\mathrm{VA}}/dA=0$, is quadratic for A^2, which yields two solutions:

$$(A^2)_{1,2} = \frac{\cosh(2\alpha\chi)}{\sinh(2\alpha)} \frac{\sinh(3\alpha)}{\cosh(3\alpha\chi)} (1 \pm \sqrt{1+\Sigma}), \tag{13}$$

$$\Sigma \equiv \left[[\mu - 2C(1 - e^{-\alpha}\cos k)] \frac{\cosh(\alpha\chi)}{\sinh(\alpha)} + 2Ce^{-\alpha}\cos k \right] \times \frac{\cosh(3\alpha\chi)}{\sinh(3\alpha)} \frac{\sinh^2(2\alpha)}{\cosh^2(2\alpha\chi)}. \tag{14}$$

Using Eq. (2) and VA ansatz (9), it is straightforward to find the corresponding soliton's norm (power), $P_{\mathrm{VA}}=A^2 S_0$. In accordance with the above analysis, the coexistence of two solitons with different norms may be expected in some regions of the (μ, C) parameter space, in the cases of the staggered and unstaggered configurations alike.

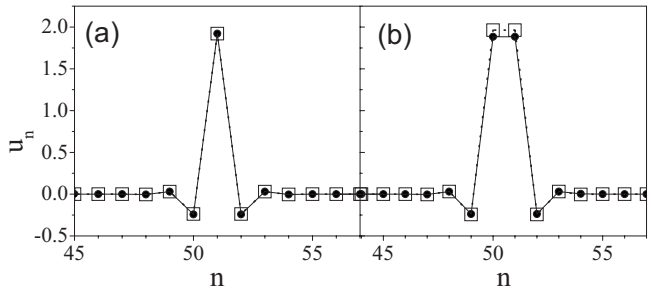

FIG. 8. Comparison of staggered soliton configurations, as generated by the numerical solution of Eq. (5), and obtained from the variational approximation based on ansatz (9), with $C=0.8$ and $\mu=8.05$, for the (a) on-site and (b) intersite configurations. The numerical and variational results are shown by dashed black curves with squares and by solid black curves with black circles, respectively.

C. Comparison of the numerical and variational results

Predictions of the VA were compared to numerical results obtained from Eq. (5). In Fig. 8, typical examples of staggered on-site and intersite solitons, generated by means of both methods, are plotted. In this case, the VA produces only one solution for both the on-site and intersite configurations [i.e., only one expression for A^2 given by Eq. (13) is positive]. It is concluded that the numerically generated on-site and inter-site solitons are almost perfectly reproduced by the VA, except for the central part of the intersite solution, where small differences can be spotted.

The numerical and variational versions of the $P(\mu)$ and $G(P)$ curves for the unstaggered and staggered solitons are very close too, in the entire (μ, C) parameter plane, as shown in Figs. 9 and 10. It is observed that the match between the numerical and variational solutions for the unstaggered discrete solitons is extremely good at small values of C and all values of μ (in the existence region), see Figs. 9(a) and 9(c), as well as at high values of C and $\mu > -0.5$, see Figs. 10(a) and 10(c). In fact, the results for the unstaggered solitons are tantamount to those reported in Ref. [26].

New findings concern the staggered discrete solitons. For the on-site configuration of these states, good matching between the numerical and variational solutions takes place in almost the entire (μ, C) plane, as seen in Figs. 9(b) and 9(d). Discrepancies for intersite staggered configurations, as observed at large values of C in Figs. 10(b) and 10(d), are explained by the irrelevance of ansatz (9) for solitons in the quasicontinuum limit [26], which corresponds to $C \to \infty$. This conclusion correlates with the findings presented in Fig. 8.

IV. MOBILITY OF THE DISCRETE BRIGHT SOLITONS

In addition to the study of the staggered discrete solitons, another major objective of this work is to study moving localized modes. Usually, in discrete systems the dynamics of motion across the lattice is interpreted in terms of the effective PNB (Peierls-Nabarro barrier) for localized states [35,36]. The PNB can be defined in a straightforward fashion

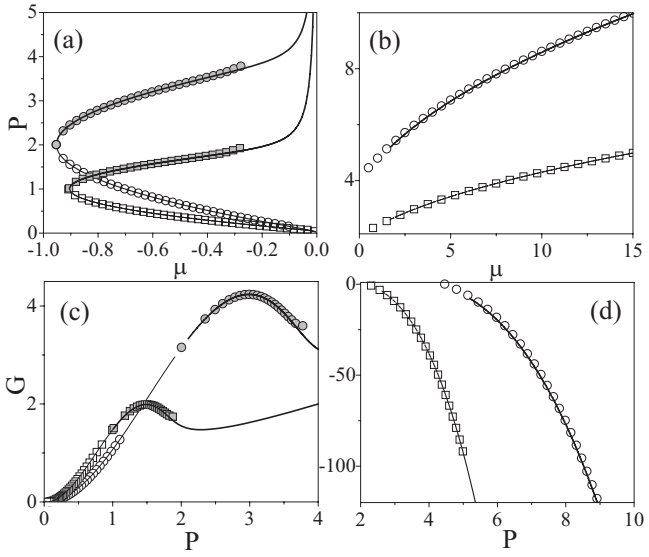

FIG. 9. $P(\mu)$ and $G(P)$ characteristics for the unstaggered and staggered discrete solitons, as generated numerically (symbols) and predicted by the variational approximation (curves), for $C=0.05$. Panels (a) and (c) correspond to unstaggered configurations, of the on-site (branch 1, open squares; branch 2, gray squares) and intersite (branch 1, open circles; branch 2, gray circles) types. The two branches for unstaggered on-site and intersite configurations correspond to the coexistence of different fundamental symmetric solitons of these types. Staggered configurations are presented in plots (b) and (d) of the on-site (curve and squares) and intersite (curve and circles) types. Note that in areas with only VA curves plotted numerical solutions are not found.

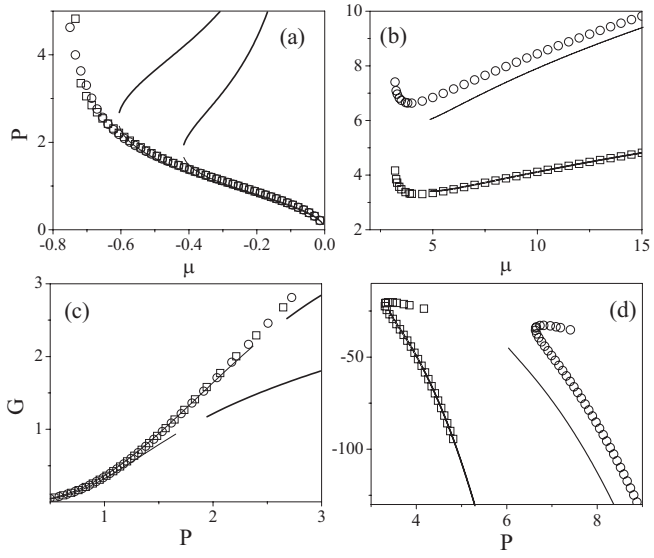

FIG. 10. Same as in Fig. 9, but for $C=0.8$ (much closer to the continuum limit). In this case, the numerical curves showing $P(\mu)$ and $G(P)$ for the on-site and intersite unstaggered configurations (squares and circles, respectively) are very close to each other (in fact, they overlap); cf. Fig. 3(a). These curves are perfectly approximated by the corresponding variational (solid) curves. In disagreement with the numerical findings which demonstrate the existence of a single symmetric fundamental unstaggered on-site and intersite soliton configuration for each μ, the variational approximation predicts two such configurations with different norms (bold and thin curves). The discrepancies between the variational and numerical results in this case are due to the irrelevance of ansatz (9) for solitons in the quasicontinuum limit.

for discrete solitons of the topological type, such as kinks in the Frenkel-Kontorova model [37] and its modification with a deformable substrate potential [38], see also book [39]. For nontopological solitons (or, generally, intrinsic localized modes), the effective PNB is only estimated as an energy barrier which has to be overcome by a localized discrete state in the lattice to allow its progressive motion. Vanishing of the so evaluated effective PNB is an indication to a possibility of persistent motion of the nontopological discrete soliton across the lattice.

The fact that the PNB, although being an intuitively clear concept, cannot be defined in a unique way was discussed in various contexts [29,30,36]. In this section, the effective PNB is estimated in the framework of two concepts, viz., free energy [28,29] and mapping analysis [30,31]. The predictions will be verified by comparison with direct numerical simulations of Eq. (1). In the simulations, the motion of the discrete soliton is initiated by applying a kick of size K, i.e., multiplying the soliton by $\exp(iKn)$.

A. Free-energy concept

The PNB is usually estimated as the difference between values of the Hamiltonian, or free energy G, for on-site ("on") and inter-site ("in") stationary localized modes with the same power (norm) or μ [29,36]. In terms of the free-energy difference for the modes with equal values of the norm, the barrier is evaluated as

$$\Delta G_{\mathrm{PN}} = G_{\mathrm{on}} - G_{\mathrm{in}} = \Delta H - P\Delta\mu, \tag{15}$$

where $\Delta H = H_{\mathrm{on}} - H_{\mathrm{in}}$, and $\Delta\mu = \mu_{\mathrm{on}} - \mu_{\mathrm{in}}$. The values of the free energy for unstaggered on-site and intersite solitons with equal norms are very close to each other at large C, hence the PNB practically vanishes for them. As a consequence, moving unstaggered solitons exist in a wide region of the parameter space (in fact, for $C > 0.2$). More precisely, an unstaggered soliton can be set in motion by the kick exceeding some threshold value at small C, or by almost any value of K at large C; see an example in Fig. 11. The unstaggered soliton remains trapped, for $K \lesssim K_{\mathrm{thr}}$, in Figs. 11(a) and 11(b) and freely moves, for $K > K_{\mathrm{thr}}$, in Fig. 11(c).

Generally, the simulations confirm the validity of the proposed PNB concept, as said above, for $C \gtrsim 0.2$. On the other hand, in the region of small C the PNB vanishes only for small μ. In accordance with this, the simulations demonstrate that moving discrete solitons cannot be created in that region, even if a very strong kick is applied to a quiescent unstaggered discrete soliton.

The numerically generated estimate of the PNB for unstaggered localized modes is presented in Fig. 12. To generate the figure, we used results of direct simulations performed on the time scale covering several hundreds periods of natural intrinsic oscillations of the discrete soliton. Persistent progressive motion of the kicked soliton is observed in

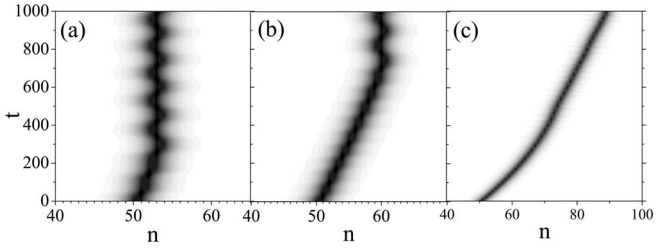

FIG. 11. Dynamics of the localized mode which is transversely kicked, i.e., the corresponding field is multiplied by e^{iKn}, for $C=0.4$. (a) The application of the kick with $K=\pi/512$ leaves the discrete soliton trapped after a very short period of initial motion; (b) $K=\pi/256$ leaves it trapped too after a longer period of the transient motion; (c) $k=\pi/32$ gives rise to a persistently moving localized state.

areas with very small ΔG ($|\Delta G|<10^{-3}$) for $C>0.4$ and all K, while, for higher ΔG, it is only observed for $K>K_{\text{thr}}$. In the latter case, the threshold value of the kick is proportional to the respective value of ΔG. The velocity of the moving soliton is found to be a linear function of the applied kick. At $C<0.4$, persistent motion was not observed (transient motion may occur, but the trapping prevails in the long-time limit). Plots in Fig. 12 show borders in the (K,μ) plane, for two fixed values of C, which separate the pinned and moving

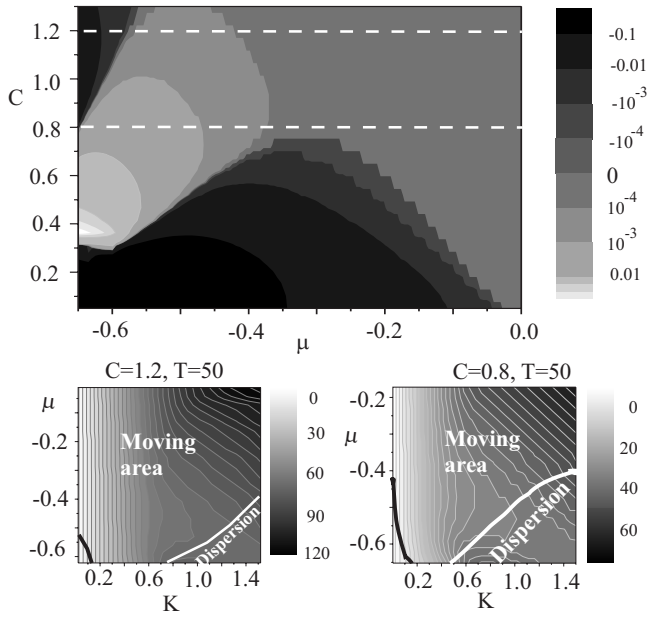

FIG. 12. In the top plot, the values of the Peierls-Nabarro barrier, ΔG, estimated as per Eq. (15) for the unstaggered soliton, are shown in the (C,μ) plane by means of the gray scale. Two bottom plots show the borders in the (K,μ) plane, for two fixed values of C corresponding to the dashed white lines in the top plot, that separate the dynamical regimes in which the kicked soliton remains pinned (the area below the bold black curve), is set in persistent motion—"moving area," or gets destroyed (the "dispersion" area below the bold white curve). The gray scale in these panels shows how many lattice cells the moving soliton has passed up to time $T=50$, which demonstrates that the velocity of the moving unstaggered soliton is a linear function of the initial kick.

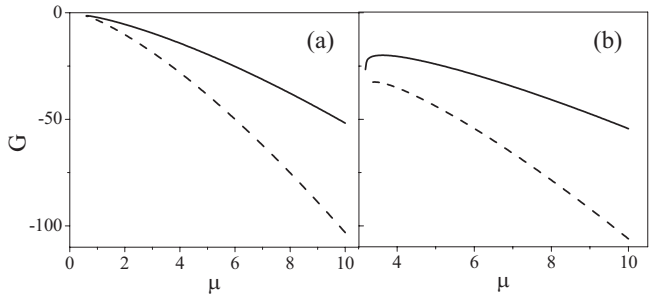

FIG. 13. $G(\mu)$ dependencies for the staggered discrete solitons at (a) $C=0.15$ and (b) $C=0.8$. The on-site and intersite configurations are represented by the solid and dashed curves, respectively.

solitons, and regimes of the stable motion and destruction of the unstaggered soliton by the strong kick ("dispersion").

As concerns staggered discrete solitons, numerical results displayed in Fig. 7 show a large difference in the norm between the states involved in definition (15), hence this definition is doubtful. A possibility may be to evaluate the PNB for staggered solitons as follows:

$$\Delta G_{\text{PN}} = G_{\text{on}} - G_{\text{in}} = \Delta H - \mu \Delta P, \tag{16}$$

where $\Delta P = P_{\text{on}} - P_{\text{in}}$, while μ is the same for both the on-site and intersite configurations [29]. The respective $G(\mu)$ dependencies are plotted for $C=0.15$ and $C=0.8$ in Fig. 13. For both values of C, curves $G(\mu)$ for the on-site and intersite localized states are clearly separated, making the PNB very high. As a consequence, the localized staggered discrete solitons *cannot* be set in the state of persistent motion.

B. Mapping analysis

It is well known that integrable discrete models, such as the Ablowitz-Ladik equation, possess exact solutions for discrete bright solitons that are manifested in the corresponding integrable map as perfect separatrices with coinciding stable and unstable manifolds of the fixed point at the map's origin [30,31]. On the other hand, in nonintegrable systems (for example, the DNLS equation) the separatrix is not perfect, in the sense that the stable and unstable manifolds no longer coincide but rather intersect each other transversely at homoclinic points, giving rise to chaotic dynamics, that eventually develop Smale-horseshoe chaotic structures. In Refs. [30,31] it was shown that dynamically stable localized structures correlate with the emergence of chaotic areas in the corresponding map.

Following the procedure developed in Ref. [26], the map corresponding to stationary equation (5) can be written as

$$u_{n+1} = (a - 2C^{-1}u_n^2 + C^{-1}u_n^4)(\cos K)^{-1}u_n - v_n, v_{n+1} = u_n,$$

with $a \equiv 2 - \mu/C$. This map possesses five fixed points:

$$u_0 = 0, \quad u_{\pm\pm} = \pm\{1 \pm \sqrt{[1 - C(a - 2\cos K)]}\},$$

where two signs $\pm$ are mutually independent.

The presence of the homoclinic orbit around $u_0=0$ indicates the existence of a bright fundamental soliton. Several

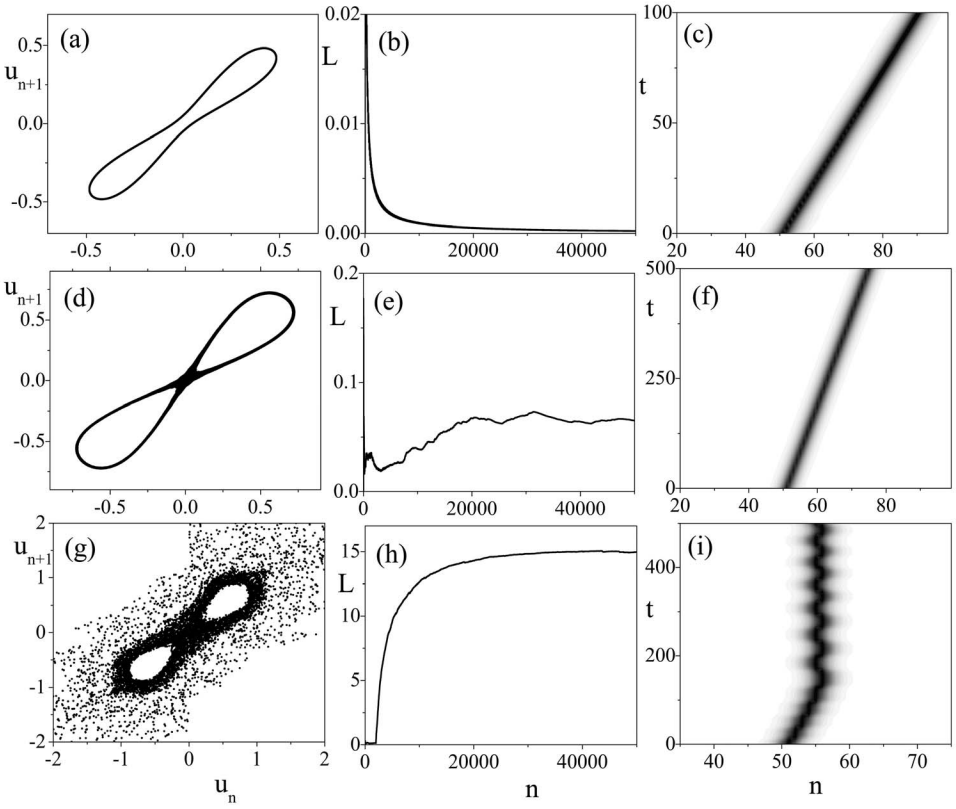

FIG. 14. Mapping of trajectories around the origin, and the corresponding Lyapunov exponents (which estimate the stochasticity of the map), for $C=0.8$, and (a), (b) $\mu=-0.202$, (d), (e) $\mu=-0.412$, and (g), (h) $\mu=-0.622$. In the case of $\mu=-0.202$ the trajectory is a perfect separatrix, and, accordingly, a moving discrete soliton is easily generated by the application of the kick, as shown in panel (c) (the size of the kick is $K=\pi/48$). A similar situation is observed in (f) for $\mu=-0.412$. The last case, with $\mu=-0.622$, is characterized by the existence of a wide stochastic layer in the map, hence a stronger kick is required to set the localized mode in initial motion, and the soliton eventually comes to a halt, as shown in panel (i) (for $K=\pi/48$).

examples are plotted in Figs. 14(a), 14(d), and 14(g). In these figures, the positive 1D Lyapunov exponent [31] is taken as a measure of the developed chaos, which is strongly related to the existence of moving localized modes as mentioned above; see Figs. 14(b), 14(e), and 14(h).

From the viewpoint of the moving localized modes, the existence of a perfect, or nearly perfect, map separatrix (proximity to the integrability) can be associated with the vanishing of the PNB [30,31]. A change from the perfect map separatrix to an imperfect one with variation of a parameter is then interpreted as an increase of the PNB.

A perfect or nearly perfect map separatrix is characteristic for some parts of the existence region for the discrete solitons. Only there persistently moving localized sates can be generated by the application of the kick; see Figs. 14(c) and 14(f). In other areas, moving localized modes exist only temporally, being eventually trapped by the lattice, see Fig. 14(i), or cannot exist at all. The latter trend correlates with the increasing stochasticity of the map, as shown in Fig. 14. In fact, this kind of the analysis fully corroborates the above conclusions concerning the motion of the kicked unstaggered solitons, as well as the inference that moving modes cannot be generated from staggered discrete solitons, as the latter ones correlate with the highly developed map stochasticity.

V. CONCLUSIONS

We have considered the dynamics of bright discrete solitons in the 1D lattice, supported by the competing on-site self-focusing cubic and self-defocusing quintic terms. While the existence and stability of unstaggered stationary solitons was studied in recent work [26], we have here presented a comprehensive analysis of the staggered solitons, performed by means of the numerical and analytical methods (the latter based on the variational approximation). The stability of the on-site and intersite staggered solitons in a large part of their existence region was established, through the computation of the stability eigenvalues. The results were confirmed by direct numerical simulations.

The main purpose of the work is the study of the moving solitons. The dynamics of the localized modes in the CQ lattice was considered in terms of the effective Peierls-Nabarro barrier (PNB), which was estimated in the framework of two concepts: Free energy and the mapping analysis. Both approaches produce consistent results, predicting that persistently moving localized modes can only be generated from the unstaggered quiescent discrete solitons. However, no moving unstaggered localized states could be found for very small values of the lattice-coupling constant, C, although the corresponding effective PNB vanishes. In fact, the behavior of the moving discrete solitons can be analyzed in a fully consistent fashion only within the framework of the mapping analysis.

The model analyzed in the paper can be developed in various directions. In particular, it may be interesting to study the discrete solitons in the lattice system where the quintic nonlinearity is self-attractive, which, as explained above, is relevant to model the self-attractive BEC trapped in a deep optical lattice. Another obviously relevant generalization may be for solitons and vortices in the two-dimensional version of the model.

Note added in proof. Recently optical CQ nonlinearity was observed in a colloidal medium [40], in agreeement with

an earlier theoretical prediction [41]. In fact, the quintic part of the nonlinearity may have either sign in that setting. These results expand possibilities for the experimental implementation of the solitons predicted in the present work.

ACKNOWLEDGMENT

A.M. and L.H. acknowledge support from the Ministry of Science of Serbia (Project No. 141034).

[1] P. G. Kevrekidis, K. Ø. Rasmussen, and A. R. Bishop, Int. J. Mod. Phys. B **15**, 2833 (2001).
[2] D. N. Christodoulides and R. I. Joseph, Opt. Lett. **13**, 794 (1988).
[3] H. S. Eisenberg, Y. Silberberg, R. Morandotti, A. R. Boyd, and J. S. Aitchison, Phys. Rev. Lett. **81**, 3383 (1998).
[4] D. N. Christodoulides, F. Lederer, and Y. Silberberg, Nature (London) **424**, 817 (2003).
[5] J. W. Fleischer, G. Bartal, O. Cohen, T. Schwartz, O. Manela, B. Freedman, M. Segev, H. Buljan, and N. K. Efremidis, Opt. Express **13**, 1780 (2005).
[6] M. J. Ablowitz, Z. H. Musslimani, and G. Biondini, Phys. Rev. E **65**, 026602 (2002).
[7] I. E. Papacharalampous, P. G. Kevrekidis, B. A. Malomed, and D. J. Frantzeskakis, Phys. Rev. E **68**, 046604 (2003).
[8] J. Meier, G. I. Stegeman, Y. Silberberg, R. Morandotti, and J. S. Aitchison, Phys. Rev. Lett. **93**, 093903 (2004); J. Meier, G. I. Stegeman, D. N. Christodoulides, R. Morandotti, M. Sorel, H. Yang, G. Salamo, J. S. Aitchison, and Y. Silberberg, Opt. Express **13**, 1797 (2005); Y. Linzon, Y. Sivan, B. Malomed, M. Zaezjev, R. Morandotti, and S. Bar-Ad, Phys. Rev. Lett. **97**, 193901 (2006).
[9] D. Cheskis, S. Bar-Ad, R. Morandotti, J. S. Aitchison, H. S. Eisenberg, Y. Silberberg, and D. Ross, Phys. Rev. Lett. **91**, 223901 (2003).
[10] A. Trombettoni and A. Smerzi, Phys. Rev. Lett. **86**, 2353 (2001); G. L. Alfimov, P. G. Kevrekidis, V. V. Konotop, and M. Salerno, Phys. Rev. E **66**, 046608 (2002); R. Carretero-González and K. Promislow, Phys. Rev. A **66**, 033610 (2002); F. S. Cataliotti, S. Burger, C. Fort, P. Maddaloni, F. Minardi, A. Trombettoni, A. Smerzi, and M. Inguscio, Science **293**, 843 (2001); M. Greiner, O. Mandel, T. Esslinger, T. W. Hänsch, and I. Bloch, Nature (London) **415**, 39 (2002); N. K. Efremidis and D. N. Christodoulides, Phys. Rev. A **67**, 063608 (2003); M. A. Porter, R. Carretero-González, P. G. Kevrekidis, and B. A. Malomed, Chaos **15**, 015115 (2005).
[11] M. Salerno, Phys. Rev. A **46**, 6856 (1992).
[12] M. J. Ablowitz and J. F. Ladik, J. Math. Phys. **17**, 1011 (1976).
[13] J. Gomez-Gardeñes, B. A. Malomed, L. M. Floria, and A. R. Bishop, Phys. Rev. E **73**, 036608 (2006); **74**, 036607 (2006).
[14] V. O. Vinetskii and N. V. Kukhtarev, Sov. Phys. Solid State **16**, 2414 (1975).
[15] M. Stepić, D. Kip, L. Hadžievski, and A. Maluckov, Phys. Rev. E **69**, 066618 (2004); L. Hadžievski, A. Maluckov, M. Stepić, and D. Kip, Phys. Rev. Lett. **93**, 033901 (2004); A. Khare, K. Ø. Rasmussen, M. R. Samuelsen, and A. Saxena, J. Phys. A **38**, 807 (2005).
[16] R. A. Vicencio and M. Johansson, Phys. Rev. E **73**, 046602 (2006).
[17] F. Chen, M. Stepić, C. E. Ruter, D. Runde, D. Kip, V. Shandarov, O. Manela, and M. Segev, Opt. Express **13**, 4314 (2005).
[18] F. Smektala, C. Quemard, V. Couderc, and A. Barthélémy, J. Non-Cryst. Solids **274**, 232 (2000); G. Boudebs, S. Cherukulappurath, H. Leblond, J. Troles, F. Smektala, and F. Sanchez, Opt. Commun. **219**, 427 (2003); C. Zhan, D. Zhang, D. Zhu, D. Wang, Y. Li, D. Li, Z. Lu, L. Zhao, and Y. Nie, J. Opt. Soc. Am. B **19**, 369 (2002).
[19] Y.-F. Chen, K. Beckwitt, F. W. Wise, and B. A. Malomed, Phys. Rev. E **70**, 046610 (2004).
[20] Kh. I. Pushkarov, D. I. Pushkarov, and I. V. Tomov, Opt. Quantum Electron. **11**, 471 (1979); Kh. I. Pushkarov and D. I. Pushkarov, Rep. Math. Phys. **17**, 37 (1980); S. Cowan, R. H. Enns, S. S. Rangnekar, and S. S. Sanghera, Can. J. Phys. **64**, 311 (1986); J. Herrmann, Opt. Commun. **87**, 161 (1992).
[21] I. M. Merhasin, B. V. Gisin, R. Driben, and B. A. Malomed, Phys. Rev. E **71**, 016613 (2005); see also works in which the cubic-quintic nonlinearity is combined with a sinusoidal one-dimensional potential: J. Wang, F. Ye, L. Dong, T. Cai, and Y.-P. Li, Phys. Lett. A **339**, 74 (2005); F. Abdullaev, A. Abdumalikov, and R. Galimzyanov, *ibid.* **367**, 149 (2007).
[22] R. Driben, B. A. Malomed, A. Gubeskys, and J. Zyss, Phys. Rev. E **76**, 066604 (2007).
[23] A. E. Muryshev, G. V. Shlyapnikov, W. Ertmer, K. Sengstock, and M. Lewenstein, Phys. Rev. Lett. **89**, 110401 (2002); L. D. Carr and J. Brand, *ibid.* **92**, 040401 (2004); Phys. Rev. A **70**, 033607 (2004); L. Khaykovich and B. A. Malomed, *ibid.* **74**, 023607 (2006).
[24] L. Salasnich, A. Parola, and L. Reatto, Phys. Rev. A **65**, 043614 (2002).
[25] J. Dorignac, J. C. Eilbeck, M. Salerno, and A. C. Scott, Phys. Rev. Lett. **93**, 025504 (2004).
[26] R. Carretero-Gonzáles, J. D. Talley, C. Chong, and B. A. Malomed, Physica D **216**, 77 (2006).
[27] E. W. Laedke, K. H. Spatschek, and S. K. Turitsyn, Phys. Rev. Lett. **73**, 1055 (1994); B. A. Malomed and M. I. Weinstein, Phys. Lett. A **220**, 91 (1996); S. Flach, K. Kladko, and R. S. MacKay, Phys. Rev. Lett. **78**, 1207 (1997).
[28] A. Maluckov, L. Hadzievski, and B. A. Malomed, Phys. Rev. E **76**, 046605 (2007).
[29] T. R. O. Melvin, A. R. Champneys, P. G. Kevrekidis, and J. Cuevas, Phys. Rev. Lett. **97**, 124101 (2006).
[30] S. Aubry, Physica D **7**, 240 (1983).
[31] A. Maluckov, L. Hadžievski, and M. Stepić, Physica D **216**, 95 (2006).
[32] L. Albuch and B. A. Malomed, Math. Comput. Simul. **74**, 312 (2007).
[33] Yu. S. Kivshar and G. P. Agrawal, *Optical Solitons: from Fibers to Photonic Crystals* (Academic, San Diego, 2003).
[34] N. G. Vakhitov and A. A. Kolokolov, Izv. Vyssh. Uchebn. Zaved., Radiofiz. **16**, 10120 (1973) [Radiophys. Quantum Electron. **16**, 783 (1973)].

[35] Yu. S. Kivshar and D. K. Campbell, Phys. Rev. E **48**, 3077 (1993).
[36] R. Morandotti, U. Peschel, J. S. Aitchison, H. S. Eisenberg, and Y. Silberberg, Phys. Rev. Lett. **83**, 2726 (1999).
[37] Y. Ishimori and T. Munakata, J. Phys. Soc. Jpn. **51**, 3367 (1982).
[38] M. Peyrard and M. Remoissenet, Phys. Rev. B **26**, 2886 (1982).
[39] T. Dauxois and M. Peyrard, *Physics of Solitons* (Cambridge University Press, Cambridge, UK, 2006).
[40] E. L. Falcão-Filho, C. B. de Araújo, and J. J. Rodrigues, Jr., J. Opt. Soc. Am. B **24**, 2948 (2007).
[41] G. S. Agarwal and S. Dutta Gupta, Phys. Rev. A **38**, 5678 (1988).